STRUCTURAL BIOLOGY COMMUNICATIONS

ISSN 2053-230X

Heterogeneous nucleation is required for crystallization of the ZnuA domain of pneumococcal AdcA

Zhenyao Luo,[a,b,c]* Jacqueline R. Morey,[d] Christopher A. McDevitt[d] and Boštjan Kobe[a,b,c]*

[a]School of Chemistry and Molecular Biosciences, The University of Queensland, St Lucia, Brisbane, Queensland 4072, Australia, [b]Institute for Molecular Bioscience, The University of Queensland, St Lucia, Brisbane, Queensland 4072, Australia, [c]Australian Infectious Diseases Research Centre, The University of Queensland, St Lucia, Brisbane, Queensland 4072, Australia, and [d]Research Centre for Infectious Diseases, School of Biological Sciences, The University of Adelaide, Adelaide, South Australia 5005, Australia. *Correspondence e-mail: uqzluo1@uq.edu.au, b.kobe@uq.edu.au

Received 17 September 2015
Accepted 10 November 2015

Edited by J. Newman, Bio21 Collaborative Crystallization Centre, Australia

Keywords: heterogeneous nucleation; seaweed; ZnuA; AdcA; Zn^{2+}; *Streptococcus pneumoniae*; solute-binding protein.

Zn^{2+} is an essential nutrient for all known forms of life. In the major human pathogen *Streptococcus pneumoniae*, the acquisition of Zn^{2+} is facilitated by two Zn^{2+}-specific solute-binding proteins: AdcA and AdcAII. To date, there has been a paucity of structural information on AdcA, which has hindered a deeper understanding of the mechanism underlying pneumococcal Zn^{2+} acquisition. Native AdcA consists of two domains: an N-terminal ZnuA domain and a C-terminal ZinT domain. In this study, the ZnuA domain of AdcA was crystallized. The initial crystals of the ZnuA-domain protein were obtained using dried seaweed as a heterogeneous nucleating agent. No crystals were obtained in the absence of the heterogeneous nucleating agent. These initial crystals were subsequently used as seeds to produce diffraction-quality crystals. The crystals diffracted to 2.03 Å resolution and had the symmetry of space group *P*1. This study demonstrates the utility of heterogeneous nucleation. The solution of the crystal structures will lead to further understanding of Zn^{2+} acquisition by *S. pneumoniae*.

1. Introduction

First-row transition-metal ions are essential for all known forms of life (Klein & Lewinson, 2011). Bacterial acquisition of essential transition metals is generally achieved by metal-specific solute-binding proteins (SBPs; Klein & Lewinson, 2011; Counago *et al.*, 2012). SBPs reside on the extracytosolic side of bacterial cells (Sutcliffe & Russell, 1995; Adler, 1975) and deliver metal-ion cargoes to specific ATP-binding cassette permeases, which then facilitate active transport of the ions across the cytoplasmic membrane (Davidson *et al.*, 2008; Rees *et al.*, 2009). The SBPs involved in the acquisition of transition-metal ions are generally defined by an overall structure comprising two globular $(\alpha/\beta)_4$ lobes, referred to as the N-terminal and C-terminal lobes, that are linked by a rigid α-helix that spans the length of the protein (Lawrence *et al.*, 1998; Li & Jogl, 2007; Loisel *et al.*, 2008; Rukhman *et al.*, 2005; Sun *et al.*, 2009). The metal-binding site is formed by the interface between the two lobes (Klein & Lewinson, 2011).

Streptococcus pneumoniae is the world's foremost bacterial pathogen and is responsible for more than one million deaths annually (McDevitt *et al.*, 2011). Zinc, among other transition metals, is an essential nutrient for the survival and virulence of *S. pneumoniae* (Coleman, 1998; Yang *et al.*, 2006; Ammendola *et al.*, 2007). Pneumococcal uptake of Zn^{2+} is facilitated by

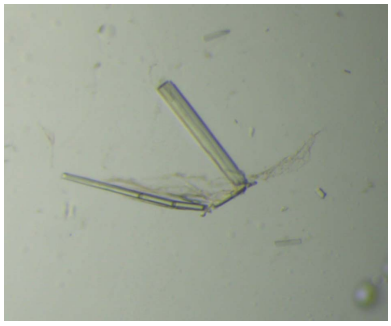

Table 1
Macromolecule-production information.

The underlined protein sequence indicates the artificial amino acids introduced by cloning. The protease cleavage sites are between the amino acids in italics.

Source organism	*S. pneumoniae* D39
DNA source	*S. pneumoniae* D39
Forward primers	
pMCSG7	5′-TACTTCCAATCCAATGCCGGTAAACTCAATA-TCGTGACAACCTTTTACCCTG-3′
pCAMnLIC01	5′-TGGGTGGTGGATTTCCTGGTAAACTCAATAT-CGTGACA-3′
Reverse primers	
pMCSG7	5′-TTATCCACTTCCAATGTTATGTTTGTTTCAA-AGCCTTGAGGTTTTTCTCC-3′
pCAMnLIC01	5′-TTGGAAGTATAAATTTCCATGCGCCAACATT-TCTTGGGC-3′
Cloning vector	pMCSG7, pCAMnLIC01
Expression vector	pMCSG7, pCAMnLIC01
Expression host	*E. coli* BL21 (DE3)
Complete amino-acid sequence of the pMCSG7 construct produced	GDIHMHHHHHHSSGVDLGTENLYF*QS*NADGKLNI-VTTFYPVYEFTKQVAGDTANVELLIGAGTEPH-EYEPSAKAVAKIQDADTFVYENENMETWVPKL-LDTLDKKKVKTIKATGDMLLLPGGEEEEGDHD-HGEEGHHHEFDPHVWLSPVRAIKLVEHIRDSL-SADYPDKKETFEKNAAAYIEKLQSLDKAYAEG-LSQAKQKSFVTQHAAFNYLALDYGLKQVAISG-LSPDAEPSAARLAELTEYVKKNKIAYIYFEEN-ASQALANTLSKEAGVKTDVLNPLESLTEEDTK-AGENYISVMEKNLKALKQTTD
Complete amino-acid sequence of the pCAMnLIC01 construct produced	MGTHHHHHHHHHHHHSAGLEVLF*QG*PGGSLGGGF-PGKLNIVTTFYPVYEFTKQVAGDTANVELLIG-AGTEPHEYEPSAKAVAKIQDADTFVYENENME-TWVPKLLDTLDKKKVKTIKATGDMLLLPGGEE-EEGDHDHGEEGHHHEFDPHVWLSPVRAIKLVE-HIRDSLSADYPDKKETFEKNAAAYIEKLQSLD-KAYAEGLSQAKQKSFVTQHAAFNYLALDYGLK-QVAISGLSPDAEPSAARLAELTEYVKKNKIAY-IYFEENASQALANTLSKEAGVKTDVLNPLESL-TEEDTKAGENYISVMEKNLKALKQTTDGNLYF-QGPWKLD

the ATP-binding cassette transporter AdcCB and the two Zn^{2+}-specific SBPs AdcA and AdcAII (Bayle *et al.*, 2011; Plumptre *et al.*, 2014). However, the lack of an experimentally determined structure of AdcA has greatly limited our understanding of its role in Zn^{2+} acquisition by *S. pneumoniae*. Sequence-alignment and secondary-structure analyses have shown that AdcA consists of two domains: an N-terminal domain (ZnuA domain), which resembles the Zn^{2+}-specific SBP ZnuA from Gram-negative bacteria, and a C-terminal domain (ZinT domain), which is homologous to ZinT, a Zn^{2+}-binding protein present in Gram-negative species. Recent studies have proposed that the ZnuA domain of AdcA acquires Zn^{2+} and initiates Zn^{2+} transport, whereas the ZinT domain of AdcA acts as a Zn^{2+} chaperone to enhance the Zn^{2+}-acquisition efficiency of AdcA during severe Zn^{2+} shortage (Plumptre *et al.*, 2014). To understand the structural basis of AdcA-facilitated Zn^{2+} acquisition in *S. pneumoniae*, crystallization of the ZnuA domain of AdcA was performed.

Initial attempts using sparse-matrix screens failed to yield any ZnuA-domain protein crystals. We hypothesized that the lack of crystals may be owing to inadequate nucleation. Nucleation is a critical and rate-limiting step in the protein crystallization process, where a nucleus of protein, aggregated in such a way as to form favourable molecular contacts, reaches a critical size. Spontaneous attachment of additional protein molecules to such a nucleus becomes energetically favourable and sizable crystals may subsequently form (Rupp, 2010). However, spontaneous nucleation often requires a specific narrow range of protein supersaturation levels, which is often difficult to locate. Furthermore, sparse-matrix screens do not sample precipitant concentration to a great extent, and the probability of spontaneous nucleation decreases with small crystallization solution volumes (Thakur *et al.*, 2007). Heterogeneous nucleation has been used as a successful approach to overcome the nucleation problem (McPherson & Shlichta, 1988; Ino *et al.*, 2011; Tosi *et al.*, 2011; Kertis *et al.*, 2012; Lin & Merlino, 2013). In heterogeneous nucleation, a material known as a heterogeneous nucleating agent, or nucleant, is introduced to the protein solution in a low supersaturated state. Heterogeneous nucleating agents have been proposed to provide structured surfaces for the formation of nuclei and to lower the thermodynamic and kinetic barriers for spontaneous nucleation (Garcia-Ruiz, 2003; Rupp, 2010). It has been shown in a number of studies that specific solid materials such as horse hair (D′Arcy *et al.*, 2003; Thakur *et al.*, 2007), porous silicon (Chayen *et al.*, 2001) and dried seaweed powder (Thakur *et al.*, 2007) can be used as heterogeneous nucleants to promote nucleation. We therefore tested dried seaweed as a heterogeneous nucleant for the crystallization of the ZnuA domain of AdcA. This approach led to diffraction-quality crystals.

2. Materials and methods

2.1. Protein production

Two different recombinant *S. pneumoniae* AdcA ZnuA-domain constructs were prepared, using the pMCSG7 and the pCAMnLIC01 vectors, to examine whether the use of different expression vectors affected protein crystallization. The pMCSG7 construct corresponded to an N-terminally hexahistidine-tagged fusion protein encoding residues 27–308 (the ZnuA domain) of AdcA. The AdcA ZnuA-domain cDNA was cloned into the pMCSG7 vector using the ligation-independent cloning technique (Eschenfeldt *et al.*, 2009). Protein expression was achieved using the auto-induction protocol (Studier, 2005), and the protein was purified using an Ni–NTA column (GE Healthcare) and a size-exclusion column (HiLoad 26/600 Superdex 75 pg, GE Healthcare). The N-terminal hexahistidine affinity tag was removed by enzymatic digestion using *tobacco etch virus* protease at a cleavage site introduced between the protein sequence and the affinity tag. The pCAMnLIC01 construct corresponded to an N-terminally dodecahistidine-tagged fusion protein encoding residues 27–321 of AdcA and was expressed and purified as described previously, with minor modifications (Plumptre *et al.*, 2014). The protein was purified using a HisTrap HP column on an ÄKTApurifier, followed by removal of the tag by enzymatic digestion by the 3C human rhinovirus protease at the cleavage site between the protein sequence and the tag. The protein was then reverse-purified

on a HisTrap HP column, with the cleaved protein eluting in the absence of imidazole. The purified protein from both constructs was concentrated to 10 mg ml^{-1} using a centrifugal filter unit (molecular-weight cutoff 10 or 30 kDa; Millipore) in a buffer solution consisting of 150 m*M* NaCl, 25 m*M* Tris pH 8.0, 5%(*v*/*v*) glycerol. Protein concentration was determined by spectrophotometry (absorbance measured at 280 nm) using a NanoDrop 2000 spectrophotometer (Thermo Scientific). The molar extinction coefficient of the protein, 30 370 M^{-1} cm^{-1}, was calculated using the *ExPASy* server (Gasteiger *et al.*, 2003). Details of the macromolecule-production information are summarized in Table 1.

2.2. Crystallization

Heterogeneous nucleation was performed using the protocol of Thakur *et al.* (2007) with minor changes. Seaweed was used as the source of the heterogeneous nucleation agent. Fresh green seaweed was purchased from a local store, washed thoroughly and dried overnight at 343 K. The dried seaweed was crushed into a fine powder with a pre-chilled mortar and pestle. During crushing, liquid nitrogen was added to the mortar to maintain the low temperature. Roughly 100 µg of the crushed seaweed powder was added to 200 µl of 10 mg ml^{-1} protein solution and the mixture was used for sparse-matrix screens and optimization experiments. Commercially available sparse-matrix screens, including Index, PEG/Ion, PEGRx (Hampton Research), Precipitant Synergy (Rigaku), JCSG, MORPHEUS, PACT and ProPlex (Molecular Dimensions), were set up at the University of Queensland Remote Operation Crystallization and X-ray Diffraction (UQ-ROCX) Facility using a Mosquito robot (TTP Labtech) in a 96-well hanging-drop vapour-diffusion plate format with 100 nl protein and 100 nl reservoir solution per drop. The plates were incubated using a Rock Imager (Formulatrix) at 293 K and the drops were monitored

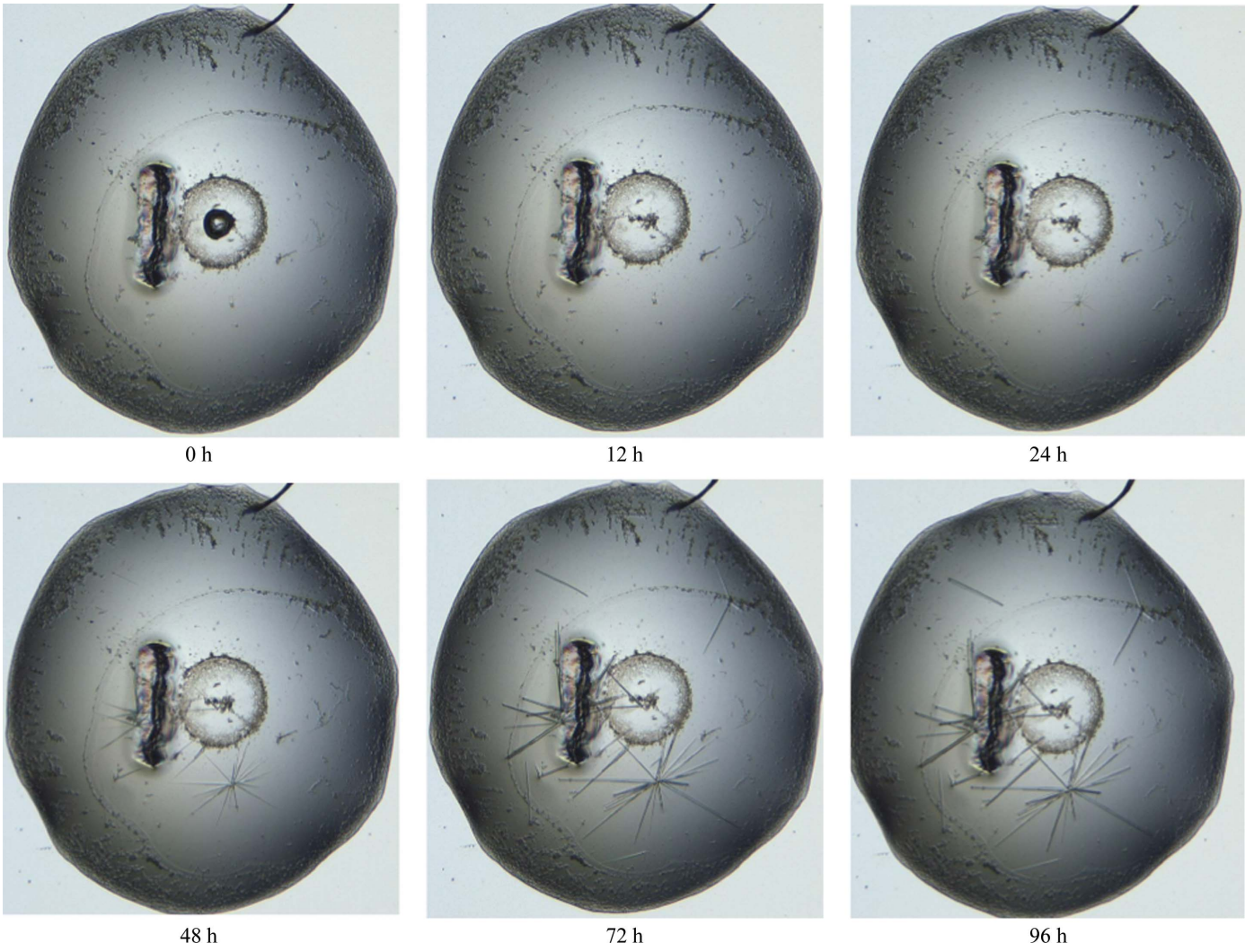

Figure 1
Crystallization of the AdcA ZnuA domain monitored from 0 to 96 h after experiment setup using MORPHEUS condition A4 [12.5%(*w*/*v*) PEG 1000, 12.5%(*w*/*v*) PEG 3350, 12.5%(*v*/*v*) 2-methyl-2,4-pentanediol, 0.03 *M* $MgCl_2$, 0.03 *M* $CaCl_2$, 0.1 *M* imidazole–MES pH 6.5] as the reservoir solution at 293 K and using dried seaweed as a heterogeneous nucleating agent. Images were obtained using the Rock Imager at the UQ-ROCX Facility at the University of Queensland.

regularly. A hit was obtained using the MORPHEUS screen, with the reservoir solution consisting of 12.5%(*w*/*v*) polyethylene glycol (PEG) 1000, 12.5%(*w*/*v*) PEG 3350, 12.5%(*v*/*v*) 2-methyl-2,4-pentanediol, 0.03 *M* $MgCl_2$, 0.03 *M* $CaCl_2$, 0.1 *M* imidazole–MES pH 6.5. The initial crystallization conditions were subjected to optimization in order to obtain diffraction-quality crystals. A series of combinations, varying the precipitant and protein concentration, the buffer pH and the incubation temperature, were explored in 24-well hanging-drop vapour-diffusion plate format. Droplets with different drop sizes were equilibrated against 1 ml reservoir solution at the chosen temperatures (277, 291 or 293 K). The micro-seeding technique was also employed using the Seed Bead kit (Hampton Research); the original needle-like crystals were collected from the crystallization drop and transferred to a pre-chilled Seed Bead tube, which is a 1.5 ml microcentrifuge tube containing a polytetrafluoroethylene bead and 50 µl crystallization solution. The Seed Bead tube was then vortexed to obtain a homogeneous solution with fine micro-crystalline seeds. Different volumes (0.2–0.5 µl) of seeds were subsequently added to the crystallization drops while setting up the plates.

2.3. Data collection and processing

Diffraction data were collected on the MX1 beamline at the Australian Synchrotron. The data set was collected using a total oscillation range of 360° with 0.5° oscillations and 1 s X-ray exposure per image. The data were indexed and integrated using *XDS* (Kabsch, 2010) and merged and scaled using *AIMLESS* from the *CCP*4 suite (Winn *et al.*, 2011; Evans & Murshudov, 2013). Initial phases were obtained by molecular replacement using *Phaser* in the *PHENIX* suite (Adams *et al.*, 2010; McCoy *et al.*, 2007) with the crystal structure of ZnuA from *Escherichia coli* (sequence identity 23%; PDB entry 2ps0; Yatsunyk *et al.*, 2008) as the search model.

3. Results and discussion

The ZnuA domain of AdcA was overexpressed in *E. coli* BL21 cells using the pMCSC7 vector and purified by immobilized metal-ion affinity chromatography and gel filtration. The N-terminal hexahistidine tag was removed by proteolysis using TEV protease prior to gel filtration. The final yield was 7 mg per litre of bacterial culture, which was sufficient for subsequent crystallization experiments. A protein concentration of 10 mg ml^{-1} was used to set up the initial sparse-matrix screens containing 100 nl protein with 100 nl reservoir solution in the drop using the hanging-drop format. The screens were prepared using a Mosquito crystallization robot (TTP Labtech) and were incubated at 293 K. However, crystallization of the ZnuA domain did not occur under any of the 768 conditions tested 21 d after experiment setup. Crystallization of a second preparation of the protein, expressed using the in pCAMnLIC01 vector, was similarly unsuccessful. The homogeneity of the protein samples was estimated to be suitable for crystallization, as indicated by the single gel band on SDS–PAGE and a narrow, symmetrical peak on gel filtration. The lack of protein crystals suggested that the conditions sampled in the initial screening may not have been suitable for spontaneous nucleation of the ZnuA-domain protein. To promote nucleation, dried seaweed powder was introduced into the initial screening drops as a heterogeneous nucleating agent, following the method suggested by Thakur *et al.* (2007). This led to successful crystallization of the protein for both constructs (Fig. 1). 24 h after experiment setup, thin needle-shaped crystals started to appear from the seaweed residuals with 12.5%(*w*/*v*) PEG 1000, 12.5%(*w*/*v*) PEG 3350, 12.5%(*v*/*v*) 2-methyl-2,4-pentanediol, 0.03 *M* $MgCl_2$, 0.03 *M* $CaCl_2$, 0.1 *M* imidazole–MES pH 6.5 (MORPHEUS condition A4) as the reservoir solution. The needle crystals of the ZnuA-domain protein were reproduced in larger scale crystallization drops (1.5 µl protein + 1.5 µl crystallization solution) using

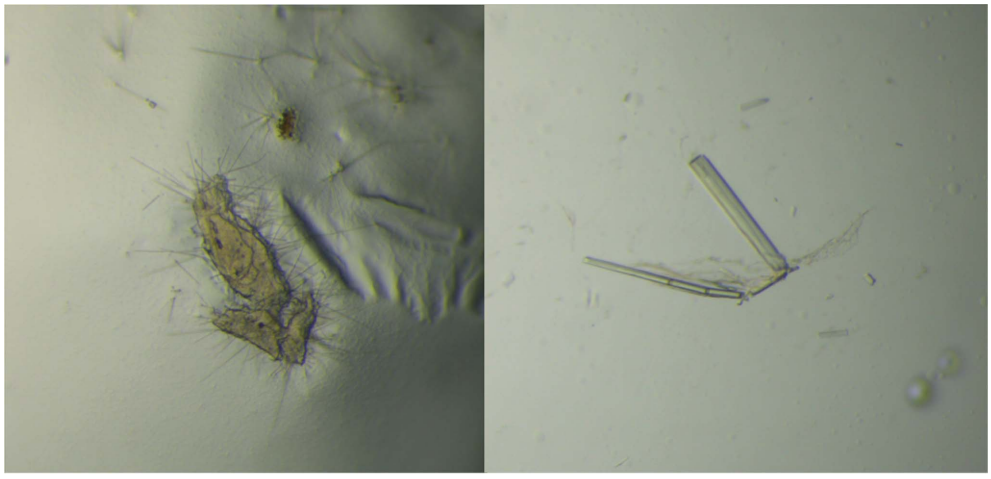

(*a*) (*b*)

Figure 2
Crystal optimization of the AdcA ZnuA domain using the micro-seeding technique. (*a*) Crystal grown on the surface of dried seaweed powder in a 3 µl crystallization drop (1.5 µl protein + 1.5 µl reservoir solution). (*b*) Crystals with improved size and shape obtained using the crystals in (*a*) as seeds. The crystals were obtained at 293 K 48 h after seeding. In both cases the reservoir solution corresponded to 12.5%(*w*/*v*) PEG 1000, 12.5%(*w*/*v*) PEG 3350, 12.5%(*v*/*v*) 2-methyl-2,4-pentanediol, 0.03 *M* $MgCl_2$, 0.03 *M* $CaCl_2$, 0.1 *M* imidazole–MES pH 6.5.

Table 2
Data collection and processing.

Values in parentheses are for the outer shell.

Diffraction source	MX1, Australian Synchrotron
Wavelength (Å)	0.954
Temperature (K)	100
Crystal-to-detector distance (mm)	300
Rotation range per image (°)	0.5
Total rotation range (°)	360
Exposure time per image (s)	1
Space group	*P*1
a, *b*, *c* (Å)	60.4, 68.0, 79.6
α, β, γ (°)	92.3, 104.7, 116.0
Mosaicity (°)	0.26
Resolution range (Å)	19.3–1.93 (2.03–1.93)
Total No. of reflections	190236 (9176)
No. of unique reflections	68710 (4604)
Completeness (%)	98.2 (97.2)
Multiplicity	3.9 (3.9)
$\langle I/\sigma(I)\rangle$	8.6 (1.9)
$R_{\rm r.i.m.}$	0.137 (1.050)
Overall *B* factor from Wilson plot (Å^2)	27.0

crystallization solution prepared in-house in the presence of dried seaweed powder. It could clearly be seen that the crystals grew on the surface of the seaweed residuals (Fig. 2*a*). These imperfect crystals were subsequently used for micro-seeding using equivalent crystallization conditions as in the original crystallization trials to obtain crystals with improved morphology and size (Fig. 2*b*). It was noted that when harvesting the initial crystals for micro-seeding, tiny pieces of seaweed in the drops could also have been picked up and the final crystals produced by a combination of homogeneous and heterogeneous nucleation. These improved crystals were then tested for diffraction at the Australian Synchrotron. The crystals diffracted to 2.03 Å resolution and a data set was collected from a single crystal. The diffraction pattern is shown in Fig. 3.

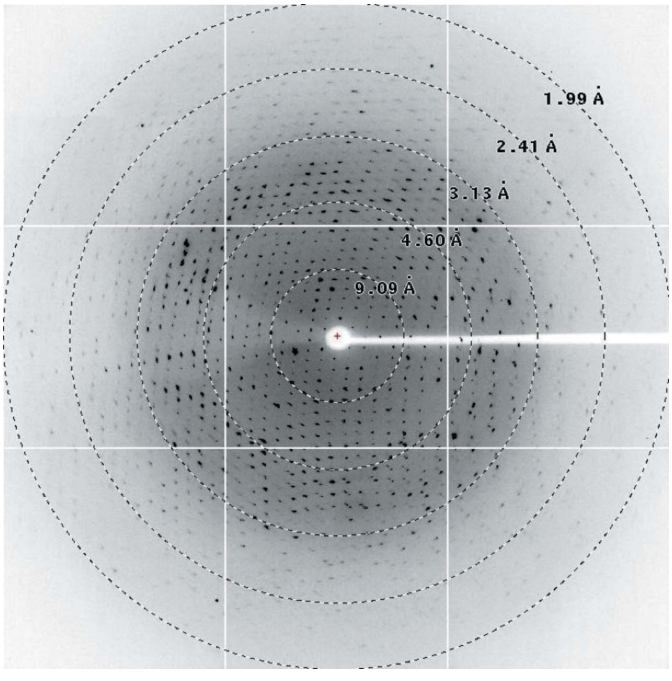

Figure 3
A representative diffraction image of the AdcA ZnuA-domain crystal. The crystal diffracted to 2.03 Å resolution. Diffraction was measured on the MX1 beamline at the Australian Synchrotron.

The ZnuA-domain crystals have the symmetry of space group *P*1, with unit-cell parameters a = 60.37, b = 67.96, c = 79.62 Å, α = 92.27, β = 104.7, γ = 116.0°. It is most likely that there are four protein molecules in the asymmetric unit, corresponding to a Matthews coefficient of 2.3 Å^3 Da^{-1} and a solvent content of 45.9%. Detailed diffraction statistics are summarized in Table 2. To obtain phase information, molecular replacement was carried out in *Phaser* with the crystal structure of Zn^{2+}-bound ZnuA from *E. coli* (PDB entry 2ps0; Yatsunyk *et al.*, 2008) as a search model. A solution was found with a translation-function *Z*-score of 21.3 and a log-likelihood gain of 7741. Structure refinement is currently in progress.

Acknowledgements

We acknowledge the use of the Australian Synchrotron MX beamlines and the UQ-ROCX Facility. We also thank Alastair McEwan and Rafael Couñago for helpful discussions and for critical review of the manuscript. This work was supported by the National Health and Medical Research Council of Australia (NHMRC) Program grants 565526 and 1071659 to BK and Project grants 1022240 and 1080784 to CAM and the Australian Research Council Discovery Project Grants DP120103957 and DP150101856 to CAM. BK is an NHMRC Research Fellow (1003326).

References

Adams, P. D. *et al.* (2010). *Acta Cryst.* D**66**, 213–221.
Adler, J. (1975). *Annu. Rev. Biochem.* **44**, 341–356.
Ammendola, S., Pasquali, P., Pistoia, C., Petrucci, P., Petrarca, P., Rotilio, G. & Battistoni, A. (2007). *Infect. Immun.* **75**, 5867–5876.
Bayle, L., Chimalapati, S., Schoehn, G., Brown, J., Vernet, T. & Durmort, C. (2011). *Mol. Microbiol.* **82**, 904–916.
Chayen, N. E., Saridakis, E., El-Bahar, R. & Nemirovsky, Y. (2001). *J. Mol. Biol.* **312**, 591–595.
Coleman, J. E. (1998). *Curr. Opin. Chem. Biol.* **2**, 222–234.
Couñago, R. M., McDevitt, C. A., Ween, M. P. & Kobe, B. (2012). *Curr. Drug Targets*, **13**, 1400–1410.
D'Arcy, A., Mac Sweeney, A. & Haber, A. (2003). *Acta Cryst.* D**59**, 1343–1346.
Davidson, A. L., Dassa, E., Orelle, C. & Chen, J. (2008). *Microbiol. Mol. Biol. Rev.* **72**, 317–364.
Eschenfeldt, W. H., Lucy, S., Millard, C. S., Joachimiak, A. & Mark, I. D. (2009). *Methods Mol. Biol.* **498**, 105–115.
Evans, P. R. & Murshudov, G. N. (2013). *Acta Cryst.* D**69**, 1204–1214.
Garcia-Ruiz, J. M. (2003). *J. Struct. Biol.* **142**, 22–31.
Gasteiger, E., Gattiker, A., Hoogland, C., Ivanyi, I., Appel, R. D. & Bairoch, A. (2003). *Nucleic Acids Res.* **31**, 3784–3788.
Ino, K., Udagawa, I., Iwabata, K., Takakusagi, Y., Kubota, M., Kurosaka, K., Arai, K., Seki, Y., Nogawa, M., Tsunoda, T., Mizukami, F., Taguchi, H. & Sakaguchi, K. (2011). *PLoS One*, **6**, e22582.
Kabsch, W. (2010). *Acta Cryst.* D**66**, 125–132.
Kertis, F., Khurshid, S., Okman, O., Kysar, J. W., Govada, L., Chayen, N. & Erlebacher, J. (2012). *J. Mater. Chem.* **22**, 21928–21934.
Klein, J. S. & Lewinson, O. (2011). *Metallomics*, **3**, 1098–1108.
Lawrence, M. C., Pilling, P. A., Epa, V. C., Berry, A. M., Ogunniyi, A. D. & Paton, J. C. (1998). *Structure*, **6**, 1553–1561.
Li, H. & Jogl, G. (2007). *J. Mol. Biol.* **368**, 1358–1366.

Lin, L.-L. & Merlino, A. (2013). *Acta Cryst.* F**69**, 669–672.
Loisel, E., Jacquamet, L., Serre, L., Bauvois, C., Ferrer, J.-L., Vernet, T., Di Guilmi, A. M. & Durmort, C. (2008). *J. Mol. Biol.* **381**, 594–606.
McCoy, A. J., Grosse-Kunstleve, R. W., Adams, P. D., Winn, M. D., Storoni, L. C. & Read, R. J. (2007). *J. Appl. Cryst.* **40**, 658–674.
McDevitt, C. A., Ogunniyi, A. D., Valkov, E., Lawrence, M. C., Kobe, B., McEwan, A. G. & Paton, J. C. (2011). *PLoS Pathog.* **7**, e1002357.
McPherson, A. & Shlichta, P. (1988). *Science*, **239**, 385–387.
Plumptre, C. D., Eijkelkamp, B. A., Morey, J. R., Behr, F., Couñago, R. M., Ogunniyi, A. D., Kobe, B., O'Mara, M. L., Paton, J. C. & McDevitt, C. A. (2014). *Mol. Microbiol.* **91**, 834–851.
Rees, D. C., Johnson, E. & Lewinson, O. (2009). *Nature Rev. Mol. Cell Biol.* **10**, 218–227.
Rukhman, V., Anati, R., Melamed-Frank, M. & Adir, N. (2005). *J. Mol. Biol.* **348**, 961–969.
Rupp, B. (2010). *Biomolecular Crystallography: Principles, Practice, and Application to Structural Biology*. New York: Garland Science.
Studier, F. W. (2005). *Protein Expr. Purif.* **41**, 207–234.
Sun, X., Baker, H. M., Ge, R., Sun, H., He, Q.-Y. & Baker, E. N. (2009). *Biochemistry*, **48**, 6184–6190.
Sutcliffe, I. C. & Russell, R. R. (1995). *J. Bacteriol.* **177**, 1123–1128.
Thakur, A. S., Robin, G., Guncar, G., Saunders, N. F. W., Newman, J., Martin, J. L. & Kobe, B. (2007). *PLoS One*, **2**, e1091.
Tosi, G., Fermani, S., Falini, G., Gavira, J. A. & Garcia Ruiz, J. M. (2011). *Cryst. Growth Des.* **11**, 1542–1548.
Winn, M. D. *et al.* (2011). *Acta Cryst.* D**67**, 235–242.
Yang, X., Becker, T., Walters, N. & Pascual, D. W. (2006). *Infect. Immun.* **74**, 3874–3879.
Yatsunyk, L. A., Easton, J. A., Kim, L. R., Sugarbaker, S. A., Bennett, B., Breece, R. M., Vorontsov, I. I., Tierney, D. L., Crowder, M. W. & Rosenzweig, A. C. (2008). *J. Biol. Inorg. Chem.* **13**, 271–288.